Nanoscale

PAPER

View Article Online
View Journal | View Issue

Cite this: *Nanoscale*, 2025, **17**, 10985

Discotic amphiphilic supramolecular polymers for drug release and cell activation with light†

Ramona Santini, ‡[a,b,c] Edgar Fuentes,‡[a] Galyna Maleeva, [a,b] Carlo Matera, §[a,b] Fabio Riefolo, ¶[a,b] José Augusto Berrocal, [d] Lorenzo Albertazzi, **[a] Pau Gorostiza *[a,b,e] and Silvia Pujals *[f]

The limited efficacy shown by drug delivery systems so far prompts the development of new molecular approaches for releasing drugs in a controlled and selective manner. Light is a privileged stimulus for delivery because it can be applied in sharp spatiotemporal patterns and is orthogonal to most biological processes. Supramolecular polymers form molecular nanostructures whose robustness, versatility, and responsivity to different stimuli have generated wide interest in materials chemistry. However, their application as drug delivery vehicles has received little attention. We built supramolecular polymers based on discotic amphiphiles that self-assemble in linear nanostructures in water. They can integrate diverse amphiphilic bioligands and release them upon illumination, acutely producing functional effects under physiological conditions. We devised two strategies for drug incorporation into the photoswitchable nanofibers. In the co-assembly strategy, discotic monomers with and without conjugated bioligands were co-assembled in helicoidal supramolecular fibers. In the drug embedding approach, we integrated a potent agonist of muscarinic receptors into the discotic polymer by noncovalent stacking interactions. This ligand can be released on demand with light *ex situ* and *in situ*, rapidly activating the target receptor and triggering intracellular responses. These novel discotic supramolecular polymers can be light-driven drug carriers for small, planar, and amphiphilic drugs.

Received 16th July 2024,
Accepted 22nd March 2025

DOI: 10.1039/d4nr02957g

rsc.li/nanoscale

Introduction

Drug delivery systems (DDSs) have emerged with the promise to selectively deliver drugs to diseased cells, allowing for more efficient treatments and lower side effects. However, despite continued efforts over the past 30 years, on average only 0.7% of the injected total dose can reach the target site.[1] Thus, finding new approaches for selective and efficient drug delivery remains an unmet need that can substantially impact modern medicine.

A powerful strategy to achieve better selectivity is using externally controlled stimuli to release DDS cargoes locally and on demand. Temperature, pH, enzyme responsiveness, and light are convenient stimuli for this purpose. Upon stimulation, DDSs readily disassemble or degrade to release their cargoes *in situ*, thus achieving higher selectivity and lower systemic toxicity than passively delivered drugs. Photorelease is one of the most promising methods, as it allows for precise spatial response and abrupt temporal jump in concentration. It avoids gradients of action (unlike temperature or pH) and takes advantage of sharp and dynamic illumination patterns with high spatiotemporal precision and technically simple means.[2,3] In addition, light is widely orthogonal to most reactions in animals.

Photorelease from hydrogels has been widely used, for example, with photocaged prodrugs,[4] but DDSs that can release drugs with light are scarcer. Reversibly photoisomerizable moieties can be used for this purpose, like azobenzenes, which stand out because of their robust photoswitching behav-

[a]*Institute for Bioengineering of Catalonia (IBEC), The Barcelona Institute for Science and Technology, Baldiri Reixac 10-12, Barcelona, 08028, Spain*
[b]*CIBER-BBN, ISCIII, Madrid, 28029, Spain*
[c]*Doctorate Program in Organic Chemistry, University of Barcelona, Carrer Martí i Franquès, Barcelona, 08028, Spain*
[d]*Institute of Chemical Research of Catalonia (ICIQ), Barcelona Institute of Science and Technology (BIST), Av. Països Catalans, 16, Tarragona, E-43007, Spain*
[e]*Catalan Institution for Research and Advanced Studies (ICREA), Barcelona, 08010, Spain. E-mail: pau@icrea.cat*
[f]*Department of Biological Chemistry, Institute for Advanced Chemistry of Catalonia, Barcelona, 08034, Spain. E-mail: silvia.pujals@iqac.csic.es*

†Electronic supplementary information (ESI) available. See DOI: https://doi.org/10.1039/d4nr02957g

‡These authors contributed equally to this work.

§Current address: Department of Pharmaceutical Sciences, University of Milan, 20133 Milan, Italy.

¶Current address: Teamit Institute, Partnerships, Barcelona Health Hub, Barcelona, 08025, Spain.

**Current address: ICMS, Eindhoven University of Technology, Eindhoven, 5600 MB, The Netherlands.

ior, biodegradability, biocompatibility, and versatility in structural design and wavelength response.[5] There is growing interest in developing photoswitchable polymers[6,7] and they have been shown to photocontrol their hydrodynamic volume, surface relief, and solid–liquid transition.[8,9]

Thus, there is a need and opportunity to develop photoswitchable polymers for temporally and spatially triggered release, and DDSs based on azobenzene appear as the most advantageous, given the favorable properties and wide knowledge of this photoisomerizable group. Supramolecular polymers (SPs) have emerged among DDSs as a novel group of molecular nanostructures with applications spanning materials chemistry, energy, and medicine. In SPs, monomers assemble into one-dimensional polymers by means of hydrophobic, electrostatic, or H-bond interactions, which make them highly dynamic modular structures.[10]

Among the different SPs, discotic amphiphiles have been instrumental for supramolecular chemists to build linear self-assembled nanostructures in water.[11,12] Their design relies on a hydrophobic core that drives self-assembly and is surrounded by three hydrophilic branches to provide aqueous solubility. The amphiphilic wedges are generally coupled to a hydrophobic C_3-symmetric core, like the well-studied 1,3,5-benzenetricarboxamide (BTA).[13] These units can stack on top of each other, creating a packed columnar aggregate, whose properties can be widely tuned in terms of length, flexibility, dynamicity, and responsiveness to different stimuli.[14–16] Such versatility underlies their success in diverse applications, from biomaterials to electronics.[13,17,18] Moreover, as they are formed by biocompatible units (amino acids and polyethylene glycol), they have shown no cytotoxic effects.[13,19,20] However, their application as drug delivery vehicles has received little attention.[21,22]

Here, we have designed a new family of BTA fibers based on monomers that exhibit reversible stability in biological media.[16,23] The BTA C_3 symmetrical core is functionalized with three amphiphilic wedges composed of different amino acid moieties, including azobenzene, octa(ethylene glycol), and lysine. These fibers are devised to respond to multiple stimuli, such as light, temperature, pH, or salt content, which can trigger their assembly or disassembly. Their stability in biological media and upon dilution was studied requiring inevitably a high stability–responsiveness trade-off.[23] Owing to the great external control on the assembly of BTA fibers, we investigated the possibilities for drug entrapment and release to activate cell membrane receptor proteins.

There are some examples of SPs with a drug attached in their monomeric units, like doxorubicin, paclitaxel, or camptothecin, in which the release is passive, *i.e.* not triggered by external stimuli.[24–30] On the other hand, there are a few examples of SPs that can assemble and disassemble by means of illumination.[16,31,32] Here, we combine for the first time drug loading and controlled disassembly to demonstrate light-triggered drug release from a SP.

Our work encompasses the design, synthesis, and characterization based on monomeric units, drug release with an external light stimulus, and, for the first time, the proof of the functional pharmacological effect of the released drug on target receptors expressed in living cells. Overall, we present a versatile system in which different types of drugs can be conveniently entrapped and released with light. We designed two strategies to load and release different biologically active ligands from a BTA-based supramolecular polymer. The first strategy, co-assembly, (Fig. 1a) aims at hydrophilic ligands and is based on a co-assembly approach in which two similar discotic monomers stack together, forming fibers. One of them carries the drug covalently attached at the hydrophilic side while the other serves as a scaffold, driving the self-assembly. For this strategy, drugs can be bulkier and non-planar as they are positioned at the edge of the wedges, which is less compact. This approach allows for loading control plus a higher loading density due to the C_3-symmetric nature of discs. The second strategy, drug embedding, (Fig. 1b) is designed for smaller and planar ligands and their direct encapsulation in the discotic planar hydrophobic pocket *via* non-covalent interactions. When choosing the ligand to be embedded, potent and planar drugs that can give π–π stacking are eligible. In both approaches, the scaffolding discotic monomer is utilized to conceal the ligands and prevent drug–receptor interactions before photorelease, thus ultimately leading to higher selectivity.

The selection of cargoes and discs is fundamental and must be carefully carried out to maximize the entrapping efficiency and to minimize the impact on self-assembly. The nomenclature used is related to the alkyl chain that merges the C_3-symmetric core with the three identical peptide-like amphiphilic wedges. C4 and C4-glut contain a 4-aminobutanoic acid linker while C8 contains an 8-aminooctanoic acid linker.[23] For strategy 1 (co-assembly), C4[23] is paired with a new bioactive monomer (C4-glut) to take advantage of the structural similarity between the two monomers (Fig. 1a). C4 is constituted by a C_3-symmetric BTA core bearing three identical amphiphilic wedges.[23] Each wedge comprises an inner hydrophobic region of azobenzene amino acids (orange in Fig. 1), which provides photo-responsiveness to the supramolecular structure (Figure S10 in the ESI†). This is followed by a 4-amino butanoic acid moiety and an octaethylene glycol (OEG) hydrophilic chain that ends in a C-terminal lysine (blue in Fig. 1). In C4-glut, the hydrophobic BTA core is maintained to maximize the co-assembly between monomers and the hydrophilic part of C4 is substituted in C4-glut by a modified glutamate group (violet in Fig. 1). We selected this important bioligand because its intrinsic anionic features at physiological pH make it hydrophilic. Glutamate is the primary excitatory neurotransmitter in the mammalian central nervous system and plays a crucial role in many neural circuits. Deregulation of glutamatergic signaling has been correlated with a wide range of disorders such as epilepsy, depression, Alzheimer's and Parkinson's diseases or unpaired vision.[33–35] The attachment point to C4 was decided to retain the activity of glutamate. It has been described how activity is retained in the case of substitutions of glutamate at the gamma carbon, yielding

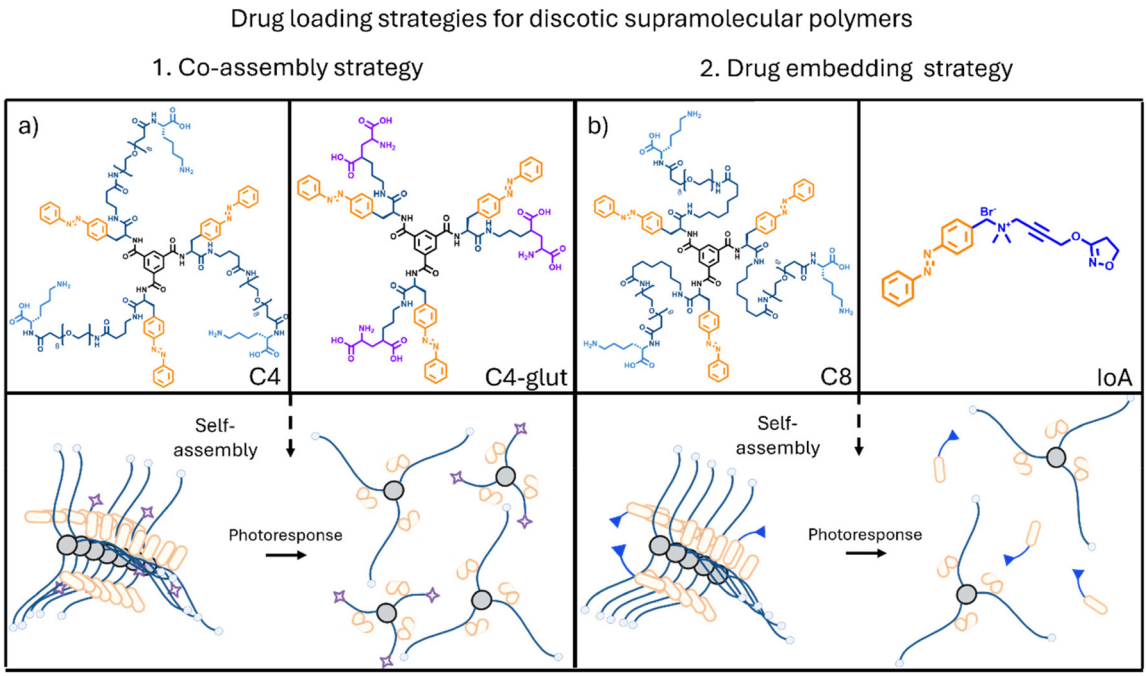

Fig. 1 Molecular structures of ligands and representation of drug loading strategies and release with light. (a) Strategy 1 (co-assembly). The left and right panels show the structures of the C4 scaffolding monomer and the C4-glut derivative containing a covalently tethered glutamate ligand, respectively. Both contain a hydrophobic core formed by three azobenzene groups (orange) and three linkers with terminal hydrophilic groups such as lysine (blue) or glutamate (violet). The bottom panel shows a diagram of the final supramolecular polymer using the same color codes and representation of the release of bioactive C4-glut upon illumination. UV light isomerizes azobenzene to a non-planar geometry that disrupts fiber stacking. (b) Strategy 2 (drug embedding). The left and right panels show the structures of the C8 scaffolding monomer and the iperoxo-azo ligand, respectively, using the same color codes as panel (a). The bottom panel shows a diagram of the final supramolecular polymer and release of freely diffusible iperoxo-azo upon UV illumination.

full agonists albeit with slightly reduced potency.[36–38] The co-assembly of C4 and C4-glut discs aims to conceal the glutamate inside the fiber shielded by OEG, thereby preventing the interaction with the receptor until light triggers the fiber's disassembly and exposure of glutamate to the medium.

For strategy 2 (drug embedding), we paired C8[23] to iperoxo-azo (IoA)[39] because of the bigger hydrophobic pocket of the C8 disc and the potential stacking interactions between phenyl-azo groups (Fig. 1b). C8 presents an equivalent structure to C4, but the 8-amino octanoic acid moiety affords a more lipophilic pocket than the 4-amino butanoic acid. Iperoxo-azo is an azobenzene derivative of the potent muscarinic acetylcholine receptor (mAChR) agonist iperoxo whose *E* and *Z* isomers exhibit equal biological activity.[39] This is in contrast to the other dualsteric azobenzene derivative of iperoxo – PhthalAzoIperoxo (PAI), which shows clear difference in biological activity between *E* and *Z* isomers.[40] Iperoxo-azo is a convenient choice for strategy 2 since its encapsulation in fibers might endow them with photoswitchable activity by means of a disassembly and release process. Iperoxo-azo is expected to stack between the *E* azobenzene units of the fibers and it should be released upon illumination with UV light, which favors non-planar (non-stacking) *Z* isomers of azobenzene. We assessed the assembly of the systems and the ligands' internalization and release using transmission electron microscopy (TEM) and circular dichroism (CD). We further confirmed the light-driven release of iperoxo-azo from the supramolecular polymer obtained by strategy 2, conducting calcium imaging experiments in cells overexpressing mAChRs.

Results and discussion

Synthesis and chemical characterization

The synthesis and chemical characterization of C4-glut are detailed in the ESI.† Briefly, the protected glutamate derivative 7 was prepared as reported[41] and coupled to Fmoc-L-phenylalanine-4 azobenzene (**8**),[42,43] followed by Fmoc deprotection under basic conditions. The product was coupled to the 1,3,5-benzenetricarbonyl trichloride core in a convergent fashion, followed by Boc deprotection (see the ESI†). Compounds C4, C8, and IoA were obtained as reported.[23,39]

Self-assembly studies

Once the molecules were synthesized (see the ESI†), the first step consisted of evaluating the co-assembly and stacking abilities of the drugs. To promote the highest entrapment, the monomers and drugs were dissolved in DMSO at high concentrations (C4: 20 mM, C4-glut: 1 mM, C8: 10 mM, and IoA:

10 mM), mixed in DMSO at the desired ratio, and injected in a specific buffer (see the details in the ESI†).

CD spectra for the two approaches (C4 + C4-glut and C8 + IoA) were obtained at different loading percentages and the characteristic peak of azobenzene assembly (250–300 nm)[16,23] was tracked (Fig. 2a and f). Internal changes were observed in both systems, decreasing slightly the characteristic stacking signal (275 nm) of azobenzene, hence indicating that IoA and C4-glut internalize in the supramolecular fibers and disturb the monomer stacking. The incorporation of C4-glut and IoA in the fibers using these bulk measurements was further investigated using microscopy.

TEM imaging was initially performed on both systems to test fiber formation and drug internalization. Fig. 2 shows the TEM images of the polymers alone, the cargoes alone, the polymers and cargoes formulated together, and the result of UV illumination (photoresponse) on the latter. Interestingly, both the "cargoes" C4-glut and IoA alone showed characteristic structures upon formulation in water (Fig. 2c and h). However, they show a more undefined and irregular bundling, very different from the morphology shown by C4 and C8 alone (Fig. 2b and g). C4-glut showed heavily aggregated structures, displaying entanglement and coiling and IoA showed thick and entangled fibers. However, when they were formulated together with C4 and C8, these characteristic morphologies were not observed (Fig. 2d and i). Instead, the fibers displayed the same characteristics as C4 and C8 alone (Fig. 2b and g). Fiber diameter analysis (ESI Fig. 11†) provides additional evidence supporting this hypothesis. The C8 and IoA mixture exhibits a unimodal diameter distribution that is distinctly different from the distributions observed for the C8 and IoA samples individually. This observation indicates that the combination of C8 and IoA results in the formation of a novel fiber type, rather than a heterogeneous mixture of fibers composed of each monomer separately. Similarly, the C4 and C4-glut mixture demonstrates a monomodal distribution that differs from the distributions of C4 and C4-glut samples in isolation. This finding suggests that the C4 and C4-glut monomers are indeed incorporated into a new composite fiber structure containing both components. Thus, these results indicate that C4-glut and IoA assemble with C4 and C8 instead of self-sorting (phase separating), and the resulting assemblies possess characteristics of the most abundant monomer (C4 or C8). If the molecules could not assemble, they would do it separately and should give rise to supramolecular polymers of both shapes.

The samples were also illuminated with UV light to trigger fiber disassembly. In the case of C4 + C4-glut (Fig. 2e), most of the fibers disappeared, leaving only a few fibers and spherical aggregates visible on the surface. These remaining aggregates may be composed of C4-glut alone, given its poor solubility both in DMSO and water, whereas C4 alone does not disassemble after illumination, as demonstrated previously.[23] In the case of C8 and IoA, the disassembly was complete upon irradiation and no aggregates were observed (Fig. 2j), thus indicating that the *Z* monomers are soluble in water and could potentially lead to IoA release to the solution, as intended.

Given these promising indications of drug incorporation into the fibers from bulk (CD) and single fiber imaging at the nanoscale (TEM), we proceeded with functional studies in cells expressing the target receptors (mAChRs) to obtain proof of the release of bioactive compounds.

Release studies

After demonstrating drug entrapment into the supramolecular fibers, we aimed to evaluate the ability to release the drug. For this purpose, the two strategies were evaluated separately.

The co-assembly strategy involving the C4 and C4-glut derivative (Fig. 1a) was tested on cultured hippocampal neurons that are known to express several types of glutamate receptors.[44] Glutamate derivatives and their pharmacological analogues (including tethered ligands) at 10–100 μM concentrations are generally capable of activating ionotropic and/or metabotropic glutamate receptors.[36,45–47] However, the application of the as-prepared (non-illuminated) fibers and UV-illuminated fibers did not produce significant fluorescence responses in calcium imaging assays using an Oregon Green BAPTA-1 chemical calcium sensor (OGB-1, see the ESI† for details). Given the low solubility of C4-glut in DMSO and the strong bundling/entanglement and aggregation in water (Fig. 2c), we hypothesize that C4-glut might be released at concentrations too low to significantly activate glutamate receptors, possibly because its hydrophobicity hampers disassembly upon isomerization. The fibers and/or spherical aggregates that are observed by TEM after UV irradiation (Fig. 2e) may be formed by C4-glut. Partially destabilizing these structures (*e.g.*, by including hydrophilic groups) might improve the performance of C4-glut.

The drug embedding strategy involving C8 and IoA (Fig. 1b) was tested on tsA201 cells overexpressing M_1 mAChRs and the genetically encoded fluorescent calcium sensor R-GECO1. Calcium-dependent fluorescence signals were recorded using a customized epifluorescence microscopy setup.[48] The C8 SP loaded with 10% mol of IoA (M_1 mAChR agonist)[39] was applied onto cells (final concentrations of C8 and IoA of 450 nM and 50 nM) in a specific temporal sequence (Fig. 3a, top) and the calcium response was recorded for each cell in the field of view and averaged to evaluate cell-to-cell response variability (see the individual cell and averaged responses in thin and thick traces, respectively, in Fig. 3a).

We first applied C8 + IoA pre-illuminated with UV light and observed an increase in intracellular calcium (R-GECO1 fluorescence) (violet bar and violet-shaded box in Fig. 3a). This increase is statistically significant (violet column in Fig. 3b) and it is due to the UV-triggered release of IoA from the fibers, which activates M_1 mAChRs.[39] The transient or oscillatory time course of the intracellular calcium responses is characteristic of mAChRs and other GPCRs.[40,49,50] After the application of pre-illuminated C8 + IoA, a washout step was used to remove the compound from the cells and reduce the calcium activity. The cells were then exposed to a C8 + IoA sample of the same composition, batch, and concentration but that had not been previously illuminated with UV light. This is indi-

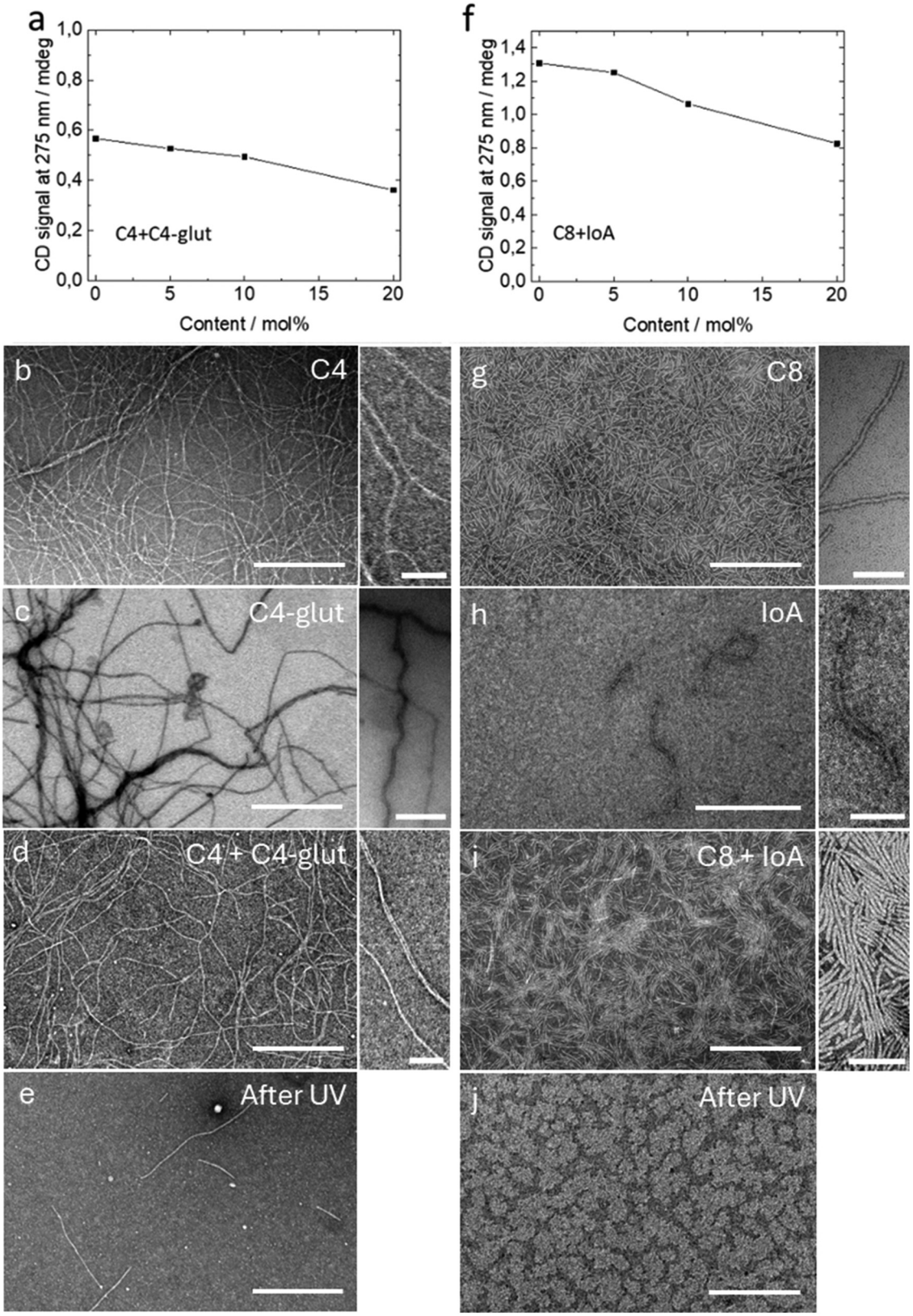

Fig. 2 CD azobenzene peak monitoring (signal at 275 nm) of system 1 (co-assembled C4 and C4-glut) (a) and drug-embedded system 2 (f) loaded at 0, 5, 10 and 20 mol% (the line was added to guide the eye). TEM imaging of the formulations to demonstrate co-assembly: C4 at 400 μM (b), C4-glut at 100 μM (c), C4 + C4-glut at 400 μM and 100 μM, respectively (d), C4 + C4-glut at 400 μM and 100 μM, respectively after UV irradiation (e), C8 at 18 μM (g), IoA at 2 μM (10 mol%) (h), C8 + IoA at 18 μM and 2 μM, respectively (i) and C8 + IoA at 18 μM and 2 μM, respectively, after UV irradiation (j). Scale bar: 500 nm, zoom in: 100 nm. Irradiation conditions: 365 nm, 1000 mA at 100% of the LED intensity for 5 min.

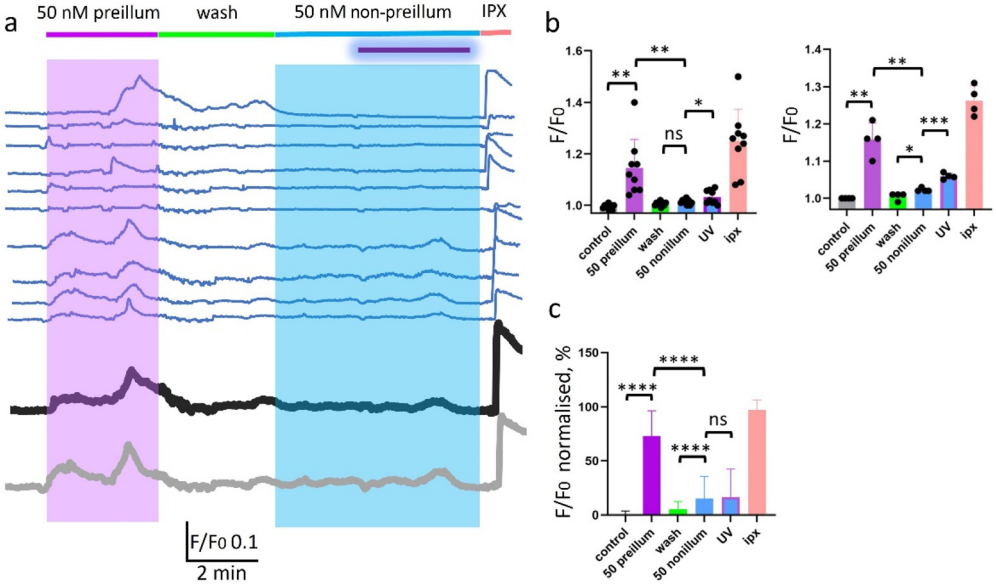

Fig. 3 Photorelease and biological activity of the entrapped IoA ligand from C8 fibers *ex situ* and *in situ*. (a) Representative traces of real-time calcium imaging responses of individual tsA201 cells expressing M_1 mAChR and R-GECO1 fluorescent calcium sensors upon application of C8 + IoA fibers under different conditions to photorelease IoA (here and for the other panels, the concentration of C8 is 450 nM and the concentration of IoA is 50 nM). The violet bar and box indicate the duration of the application of UV-pre-illuminated C8 + IoA fibers (released). The blue bar and box indicate the duration of the application of non-illuminated C8 + IoA fibers (encapsulated). *In situ* UV illumination to trigger IoA release is indicated by a violet bar. Application of 20 pM iperoxo agonist (IPX) is indicated by a red bar. The thick black trace near the bottom represents the average response of the above 10 cells. The thick gray trace depicts the averaged trace of cells responding to *in situ* UV illumination (4 last thin blue traces). (b) Left: quantification of the mean amplitude of the change of R-GECO1 fluorescence intensity (intracellular calcium activity of M_1 mAChR expressing cells) under the different conditions shown in panel (a): prior to compound application (negative control conditions, grey column), adding UV-pre-illuminated C8 + IoA fibers (violet column), washing out (green column), adding non-pre-illuminated C8 + IoA fibers before (blue column) and after UV illumination *in situ* (violet-framed blue column), and applying iperoxo (positive control conditions, red column). Significant photoresponses are observed upon *ex situ* and *in situ* UV illumination. The left panel quantification includes the traces from all cells in panel (a) (mean ± SD, n = 10 cells, and * – $P < 0.05$; ** – $P < 0.01$; ns – not significant according to the paired t-test). Right: quantification of the intracellular calcium activity of cells that responded to *in situ* UV-induced IoA release in panel (a). The statistical significance is higher than in the left plot (mean ± SD, n = 4 cells, and * – $P < 0.05$; ** – $P < 0.01$; *** – $P < 0.001$ according to the paired t-test). (c) Quantification of the increase of the calcium-dependent fluorescence signal (normalized to the maximum response of each cell) upon application of C8 + IoA fibres under different conditions to photorelease IoA. In all three independent experiments, *ex situ* release was highly significant and reaching ~80% of iperoxo responses by direct application (mean ± SD, n = 70 cells, N = 5 independent experiments, and **** – $P < 0.0001$; ns – not significant according to the paired t-test).

cated by a blue bar and blue-shaded box labeled "50 nM non-preillum" in Fig. 3a and quantified in Fig. 3b. No significant responses were observed in the ensemble of cells (blue column in Fig. 3b). After the cells were bathed in non-illuminated fibers for 3 min, we applied UV light to trigger the release of the IoA *in situ*. A fraction of cells responded with an elevation of R-GECO1 fluorescence, as shown in the four last thin traces and the thick gray trace averaging them in Fig. 3a. These responses were significant both in the ensemble of cells (violet-framed blue box in Fig. 3b, left panel) and when quantifying only the UV-responding cells (violet-framed blue box in Fig. 3b, right panel). In the second case, a minor yet statistically significant increase in activity was observed upon application of *non*-pre-illuminated C8 + IoA (prior to UV irradiation), indicating that the assembled fibers contain a fraction of free IoA that activates mAChRs. We finally applied the potent mAChR agonist iperoxo (IPX) to confirm the functionality and to estimate the expression of the receptors and observed an abrupt increase of Ca^{2+}-dependent fluorescence indicative of the maximum mAChR response in each cell. The quantification of normalized fluorescence responses from 70 cells from 5 independent experiments (Fig. 3c) shows responses to UV-pre-illuminated fibers that are high (reaching ~80% of 20 pM iperoxo response) and highly significant compared to the non-pre-illuminated ones.

Overall, the high sensitivity of calcium fluorescence assays demonstrates that IoA can be efficiently photoreleased from the C8 + IoA fibers *ex* and *in situ* (the former showing higher efficiency under our experimental conditions) and that, for the first time, our novel DDS based on discotic amphiphilic supramolecular polymers is usable in functional assays with living cells. Improving the *in situ* illumination conditions in cell assays should afford nearly complete release of the fiber cargo, as shown *ex situ*. *In situ* UV illumination of tsA201 cells expressing M_1 AChR and R-GECO1 under the control conditions, without pre-application of C8 fibers with the entrapped IoA ligand, does not produce an increase in the intensity of calcium-dependent fluorescence (ESI Fig. 12†).

We have studied two strategies for drug photorelease using azobenzene-based supramolecular polymers: co-assembly (C4 + C4-glut) and direct encapsulation of a drug in the SP hydrophobic pocket (C8 + IoA). Although the aqueous solubility of C4-glut precluded the effective photorelease in neurons, remarkable morphological and structural features were observed by CD and TEM. C4 and C4-glut alone form supramolecular fibers of different morphologies. Interestingly, C4-glut alone forms entangled supramolecular structures, which are not observed when it co-assembles with C4, proving that C4-glut is internalized into the fibers. This indicates that BTA-azo-monomers modified with a biologically active motif can be used to conceal active components into the supramolecular structure and to release them upon illumination. In this case, aqueous solubility must be taken into account and the monomer should be built with hydrophilic components (*e.g.*, glycol chains). Active components with high potency (*e.g.*, nanomolar) are also preferred if available for the target of interest because they are less dependent on solubility. Thus, the co-assembly approach is feasible, compatible with most endogenous neurotransmitters and modulators (which are hydrophilic owing to their carboxy and amino groups) and offers plenty of room for functional improvement in future designs.

The strategy of direct encapsulation of a drug in the SP hydrophobic pocket (C8 + IoA) has led to a novel light-driven DDS. Fig. 3 shows that the nanomolar active muscarinic agonist IoA is entrapped into the C8 supramolecular assembly and light can selectively trigger its release *ex situ* and *in situ*. This indicates that the BTA-azo SP can be used as a DDS for small, planar, and amphiphilic drugs capable of stacking between the monomers. Moreover, using the BTA-azo-SP is a convenient strategy to photorelease photoswitchable drugs whose isomers show limited or no difference in activity (such as IoA[39]). Thus, simple azobenzene-tethered drugs are straightforward candidates for BTA-azo SP encapsulation and photorelease, regardless of their photoswitchable activity.

Light-controlled DDSs are very desirable and several examples have been reported, like the release of doxorubicin from gold NPs,[51] doxorubicin and curcumin from polymeric NPs,[52] or chlorambucil from organic NPs.[53] Some of them are based on azobenzene, such as liposomes containing glycolipid and azobenzene to photorelease doxorubicin,[54] polymeric spherical NPs to release doxorubicin by a combination of pH and UV triggers,[55] spherical azobenzene-PEG nanostructures that photorelease 5-FU and eosin,[56] and supramolecular aptamer nano-constructs for light-triggered release of doxorubicin.[57] Regarding SPs, a polymer was reported to change their conformation from circular to linear under UV[31] and a BTA-based SP was used as a platform for the intracellular delivery of NileRed and siRNA.[22] However, a SP that can load active molecules and release them with light has never been reported.

An interesting demonstration of drug release with multiple stimuli was achieved with a coumarin-based SP.[58] Light induces dynamic covalent bonds (coumarin photodimerization) that reversibly switch the SP morphology from spherical NPs to supramolecular network assemblies and release doxorubicin, rhein or vitamin E. However, their activity was not assessed in a biological system.

The results of loading and light-triggered release of IoA (Fig. 2 and 3) are encouraging and indicate that the BTA-based SP can be used as a light-activated DDS of drugs capable of stacking with the azobenzene moieties of columnar aggregates. Importantly, small molecule encapsulation in stacked aggregates does not alter fiber properties and delivers the active molecule to living cells with nearly full efficacy. In addition, drug loading can be conveniently controlled with the C8:IoA stoichiometry and the drug-monomer geometry is better defined than in spherical micelles and NPs and the fiber polydispersity is lower.

As with other DDSs, drugs embedded into nanofibers are expected to have longer circulation times and avoid renal clearance, compared with the drug alone. Compared to small molecular weight drugs, nano-sized structures, such as the nanofibers used here, are supposed to get accumulated in inflamed tissues by passive targeting, the so-called enhanced permeability and retention (EPR) effect.[59] Together with the controlled and sustained drug release, this will lead to higher efficacy and selectivity. The system presented here shows high modularity of ligands and it could be applied to other SP systems and photoswitches. While most DDSs found in the literature encapsulate doxorubicin, our system presents two versatile strategies where many different types of drugs could be entrapped: hydrophobic/hydrophilic, planar/non-planar, bulky, *etc*.

Since non-substituted azobenzene groups require high-energy UV stimulation,[60] different triggers (like pH and light[55]) are combined in typical DDSs with spherical morphology and cargo encapsulation at the DDS core. In contrast, the disassembly of our fibers may require lower energy and propagate faster than in isolated micelles or spherical structures (where many bonds collectively support the nanostructure) because the linear structure of the fibers is supported by noncovalent bonds formed between single discotic molecules. In addition, the drug shows activity without the need for bond cleavage from the monomer. Thus, our SP DDSs allow an easier and more reversible on/off process. Further optimization of the discotic SP presented here can be achieved using red-shifted azobenzene cores[5,61–63] to reduce both the energy required for isomerization and light scattering at longer wavelengths, thus increasing the penetration depth in tissue.

Conclusions

In conclusion, we envisioned two strategies for photorelease of drugs from BTA-based supramolecular polymers: co-assembly (C4 + C4-glut) and direct encapsulation of a drug in the SP hydrophobic pocket (C8 + IoA). From the first one, we observed remarkable morphological and structural features by CD and TEM, thus confirming that BTA-azo-monomers covalently bound to active motifs can be used to include active components into the supramolecular structure and to release them

upon illumination. This shows that the co-assembly approach is feasible and can be used with other functional ligands. The strategy of direct encapsulation of a drug in the SP hydrophobic pocket (C8 + IoA) has led to a novel light-driven DDS that achieves direct activation of mAChRs upon UV illumination of the SP. This is the first example of a BTA-SP encapsulating an active ligand and releasing it upon illumination. This demonstration paves the way to encapsulate a wide range of small, planar and amphiphilic drugs capable of stacking between the monomers.

Data availability

The data supporting this article have been included as part of the ESI.†

The datasets generated and analyzed during the current study are available from the corresponding author on reasonable request.

Conflicts of interest

There are no conflicts to declare.

Acknowledgements

The authors wish to thank Unai Elezcano and Sònia Varon for help with the synthesis and purification. The authors wish to thank Isabel Oliveira and David Izquierdo for the support and useful discussion. This research was funded by the EU Horizon 2020 Framework Programme for Research and Innovation, including the European Innovation Council Pathfinder (Phototheraport, 101130883), the Human Brain Project (WaveScalES, SGA3, 945539), and Information and Communication Technologies (Deeper, ICT-36-2020-101016787); by the Government of Catalonia (CERCA Programme; AGAUR 2021-SGR-01410); by the Spanish Ministry of Science and Innovation (DEEP RED, grant PID2019-111493RB-I00; EPILLUM, grant AEI/10.13039/501100011033; STROMATARGET, grant PID2019-109450RB-I00/AEI/10.13039/501100011033; Research Network in Biomedicine eBrains-Spain, RED2022-134823-E; Ramón y Cajal Investigator grant RYC2021-033056-I financed by MCIN/AEI/10.13039/501100011033 and European Union NextGenerationEU/PRTR to G. M.); and by the Erasmus + Unipharma Graduates Programme to R. S. .

References

1 S. Wilhelm, A. J. Tavares, Q. Dai, S. Ohta, J. Audet, H. F. Dvorak and W. C. W. Chan, Analysis of Nanoparticle Delivery to Tumours, *Nat. Rev. Mater.*, 2016, **1**(5), 1–12, DOI: **10.1038/natrevmats.2016.14**.

2 C. Alvarez-Lorenzo, L. Bromberg and A. Concheiro, Light-Sensitive Intelligent Drug Delivery Systems, *Photochem. Photobiol.*, 2009, **85**(4), 848–860, DOI: **10.1111/j.1751-1097.2008.00530.x**.

3 C. S. Linsley and B. M. Wu, Recent Advances in Light-Responsive on-Demand Drug-Delivery Systems, *Ther. Delivery*, 2017, **8**(2), 89–107, DOI: **10.4155/tde-2016-0060**.

4 L. Josa-Culleré and A. Llebaria, In the Search for Photocages Cleavable with Visible Light: An Overview of Recent Advances and Chemical Strategies, *ChemPhotoChem*, 2021, **5**(4), 296–314, DOI: **10.1002/cptc.202000253**.

5 F. A. Jerca, V. V. Jerca and R. Hoogenboom, Advances and Opportunities in the Exciting World of Azobenzenes, *Nat. Rev. Chem.*, 2022, **6**(1), 51–69, DOI: **10.1038/s41570-021-00334-w**.

6 M. Clerc, S. Sandlass, O. Rifaie-Graham, J. A. Peterson, N. Bruns, J. R. Alaniz and L. F. de Boesel, Visible Light-Responsive Materials: The (Photo)Chemistry and Applications of Donor–Acceptor Stenhouse Adducts in Polymer Science, *Chem. Soc. Rev.*, 2023, **52**(23), 8245–8294, DOI: **10.1039/D3CS00508A**.

7 J. Li, Q.-Y. Zhang and X.-B. Lu, Azopolyesters with Intrinsic Crystallinity and Photoswitchable Reversible Solid-to-Liquid Transitions, *Angew. Chem., Int. Ed.*, 2023, **62**(46), e202311158, DOI: **10.1002/anie.202311158**.

8 E. Ishow, B. Lebon, Y. He, X. Wang, L. Bouteiller, L. Galmiche and K. Nakatani, Structural and Photoisomerization Cross Studies of Polar Photochromic Monomeric Glasses Forming Surface Relief Gratings, *Chem. Mater.*, 2006, **18**(5), 1261–1267, DOI: **10.1021/cm052176b**.

9 L. D. Thai, J. Fanelli, R. Munaweera, M. L. O'Mara, C. Barner-Kowollik and H. Mutlu, Main-Chain Macromolecular Hydrazone Photoswitches, *Angew. Chem., Int. Ed.*, 2024, **63**(4), e202315887, DOI: **10.1002/anie.202315887**.

10 T. Aida, E. W. Meijer and S. I. Stupp, Functional Supramolecular Polymers, *Science*, 2012, **335**(6070), 813–817, DOI: **10.1126/science.1205962**.

11 T. F. A. De Greef and E. W. Meijer, Supramolecular Polymers, *Nature*, 2008, **453**(7192), 171–173, DOI: **10.1038/453171a**.

12 E. Krieg, M. M. C. Bastings, P. Besenius and B. Rybtchinski, Supramolecular Polymers in Aqueous Media, *Chem. Rev.*, 2016, **116**(4), 2414–2477, DOI: **10.1021/acs.chemrev.5b00369**.

13 S. Varela-Aramburu, G. Morgese, L. Su, S. M. C. Schoenmakers, M. Perrone, L. Leanza, C. Perego, G. M. Pavan, A. R. A. Palmans and E. W. Meijer, Exploring the Potential of Benzene-1,3,5-Tricarboxamide Supramolecular Polymers as Biomaterials, *Biomacromolecules*, 2020, **21**(10), 4105–4115, DOI: **10.1021/acs.biomac.0c00904**.

14 K. E. Broaders, S. J. Pastine, S. Grandhe and J. M. J. Fréchet, Acid-Degradable Solid-Walled Microcapsules for pH-Responsive Burst-Release Drug Delivery, *Chem. Commun.*, 2011, **47**(2), 665–667, DOI: **10.1039/C0CC04190D**.

15 P. Ahlers, H. Frisch, R. Holm, D. Spitzer, M. Barz and P. Besenius, Tuning the pH-Switch of Supramolecular Polymer Carriers for siRNA to Physiologically Relevant pH, *Macromol. Biosci.*, 2017, **17**(10), 1700111, DOI: **10.1002/mabi.201700111**.

16 E. Fuentes, M. Gerth, J. A. Berrocal, C. Matera, P. Gorostiza, I. K. Voets, S. Pujals and L. Albertazzi, An Azobenzene-Based Single-Component Supramolecular Polymer Responsive to Multiple Stimuli in Water, *J. Am. Chem. Soc.*, 2020, **142**(22), 10069–10078, DOI: **10.1021/jacs.0c02067**.

17 P. Besenius, J. L. M. Heynens, R. Straathof, M. M. L. Nieuwenhuizen, P. H. H. Bomans, E. Terreno, S. Aime, G. J. Strijkers, K. Nicolay and E. W. Meijer, Paramagnetic Self-Assembled Nanoparticles as Supramolecular MRI Contrast Agents: SUPRAMOLECULAR MEDICINE, *Contrast Media Mol. Imaging*, 2012, **7**(3), 356–361, DOI: **10.1002/cmmi.498**.

18 N. M. Casellas, I. Urbanaviciute, T. D. Cornelissen, J. A. Berrocal, T. Torres, M. Kemerink and M. García-Iglesias, Resistive Switching in an Organic Supramolecular Semiconducting Ferroelectric, *Chem. Commun.*, 2019, **55**(60), 8828–8831, DOI: **10.1039/C9CC02466B**.

19 D. Straßburger, N. Stergiou, M. Urschbach, H. Yurugi, D. Spitzer, D. Schollmeyer, E. Schmitt and P. Besenius, Mannose-Decorated Multicomponent Supramolecular Polymers Trigger Effective Uptake into Antigen-Presenting Cells, *ChemBioChem*, 2018, **19**(9), 912–916, DOI: **10.1002/cbic.201800114**.

20 L. Li, L. Wu, M. Urschbach, D. Straßburger, X. Liu, P. Besenius and G. Chen, Modular Platform of Carbohydrates-Modified Supramolecular Polymers Based on Dendritic Peptide Scaffolds, *ACS Polym. Au*, 2022, **2**(6), 478–485, DOI: **10.1021/acspolymersau.2c00032**.

21 K. Petkau-Milroy, M. H. Sonntag, A. H. A. M. van Onzen and L. Brunsveld, Supramolecular Polymers as Dynamic Multicomponent Cellular Uptake Carriers, *J. Am. Chem. Soc.*, 2012, **134**(19), 8086–8089, DOI: **10.1021/ja3029075**.

22 M. H. Bakker, C. C. Lee, E. W. Meijer, P. Y. W. Dankers and L. Albertazzi, Multicomponent Supramolecular Polymers as a Modular Platform for Intracellular Delivery, *ACS Nano*, 2016, **10**(2), 1845–1852, DOI: **10.1021/acsnano.5b05383**.

23 E. Fuentes, Y. Gabaldón, M. Collado, S. Dhiman, J. A. Berrocal, S. Pujals and L. Albertazzi, Supramolecular Stability of Benzene-1,3,5-Tricarboxamide Supramolecular Polymers in Biological Media: Beyond the Stability-Responsiveness Trade-Off, *J. Am. Chem. Soc.*, 2022, **144**(46), 21196–21205, DOI: **10.1021/jacs.2c08528**.

24 A. G. Cheetham, P. Zhang, Y. Lin, L. L. Lock and H. Cui, Supramolecular Nanostructures Formed by Anticancer Drug Assembly, *J. Am. Chem. Soc.*, 2013, **135**(8), 2907–2910, DOI: **10.1021/ja3115983**.

25 A. G. Cheetham, P. Zhang, Y.-A. Lin, R. Lin and H. Cui, Synthesis and Self-Assembly of a Mikto-Arm Star Dual Drug Amphiphile Containing Both Paclitaxel and Camptothecin, *J. Mater. Chem. B*, 2014, **2**(42), 7316–7326, DOI: **10.1039/C4TB01084A**.

26 Z. Chen, P. Zhang, A. G. Cheetham, J. H. Moon, J. W. Moxley, Y. Lin and H. Cui, Controlled Release of Free Doxorubicin from Peptide–Drug Conjugates by Drug Loading, *J. Controlled Release*, 2014, **191**, 123–130, DOI: **10.1016/j.jconrel.2014.05.051**.

27 Y.-A. Lin, A. G. Cheetham, P. Zhang, Y.-C. Ou, Y. Li, G. Liu, D. Hermida-Merino, I. W. Hamley and H. Cui, Multiwalled Nanotubes Formed by Catanionic Mixtures of Drug Amphiphiles, *ACS Nano*, 2014, **8**(12), 12690–12700, DOI: **10.1021/nn505688b**.

28 H. Su, W. Zhang, H. Wang, F. Wang and H. Cui, Paclitaxel-Promoted Supramolecular Polymerization of Peptide Conjugates, *J. Am. Chem. Soc.*, 2019, **141**(30), 11997–12004, DOI: **10.1021/jacs.9b04730**.

29 H. Su, F. Wang, Y. Wang, A. G. Cheetham and H. Cui, Macrocyclization of a Class of Camptothecin Analogues into Tubular Supramolecular Polymers, *J. Am. Chem. Soc.*, 2019, **141**(43), 17107–17111, DOI: **10.1021/jacs.9b09848**.

30 R. Lin, A. G. Cheetham, P. Zhang, Y. Lin and H. Cui, Supramolecular Filaments Containing a Fixed 41% Paclitaxel Loading, *Chem. Commun.*, 2013, **49**(43), 4968–4970, DOI: **10.1039/C3CC41896K**.

31 S. Yagai, Y. Goto, X. Lin, T. Karatsu, A. Kitamura, D. Kuzuhara, H. Yamada, Y. Kikkawa, A. Saeki and S. Seki, Self-Organization of Hydrogen-Bonding Naphthalene Chromophores into J-Type Nanorings and H-Type Nanorods: Impact of Regioisomerism, *Angew. Chem., Int. Ed.*, 2012, **51**(27), 6643–6647, DOI: **10.1002/anie.201201436**.

32 B. Adhikari, K. Aratsu, J. Davis and S. Yagai, Photoresponsive Circular Supramolecular Polymers: A Topological Trap and Photoinduced Ring-Opening Elongation, *Angew. Chem., Int. Ed.*, 2019, **58**(12), 3764–3768, DOI: **10.1002/anie.201811237**.

33 A. Reiner and J. Levitz, Glutamatergic Signaling in the Central Nervous System: Ionotropic and Metabotropic Receptors in Concert, *Neuron*, 2018, **98**(6), 1080–1098, DOI: **10.1016/j.neuron.2018.05.018**.

34 K. B. Hansen, L. P. Wollmuth, D. Bowie, H. Furukawa, F. S. Menniti, A. I. Sobolevsky, G. T. Swanson, S. A. Swanger, I. H. Greger, T. Nakagawa, C. J. McBain, V. Jayaraman, C.-M. Low, M. L. Dell'Acqua, J. S. Diamond, C. R. Camp, R. E. Perszyk, H. Yuan and S. F. Traynelis, Structure, Function, and Pharmacology of Glutamate Receptor Ion Channels, *Pharmacol. Rev.*, 2021, **73**(4), 1469–1658, DOI: **10.1124/pharmrev.120.000131**.

35 B. S. Meldrum, Glutamate as a Neurotransmitter in the Brain: Review of Physiology and Pathology, *J. Nutr.*, 2000, **130**(4), 1007S–1015S, DOI: **10.1093/jn/130.4.1007S**.

36 M. Volgraf, P. Gorostiza, R. Numano, R. H. Kramer, E. Y. Isacoff and D. Trauner, Allosteric Control of an Ionotropic Glutamate Receptor with an Optical Switch, *Nat. Chem. Biol.*, 2006, **2**(1), 47–52, DOI: **10.1038/nchembio756**.

37 M. Volgraf, P. Gorostiza, S. Szobota, M. R. Helix, E. Y. Isacoff and D. Trauner, Reversibly Caged Glutamate: A Photochromic Agonist of Ionotropic Glutamate Receptors, *J. Am. Chem. Soc.*, 2007, **129**(2), 260–261, DOI: **10.1021/ja067269o**.

38 M. Gascón-Moya, A. Pejoan, M. Izquierdo-Serra, S. Pittolo, G. Cabré, J. Hernando, R. Alibés, P. Gorostiza and F. Busqué, An Optimized Glutamate Receptor Photoswitch

with Sensitized Azobenzene Isomerization, *J. Org. Chem.*, 2015, **80**(20), 9915–9925, DOI: **10.1021/acs.joc.5b01402**.

39 L. Agnetta, M. Bermudez, F. Riefolo, C. Matera, E. Claro, R. Messerer, T. Littmann, G. Wolber, U. Holzgrabe and M. Decker, Fluorination of Photoswitchable Muscarinic Agonists Tunes Receptor Pharmacology and Photochromic Properties, *J. Med. Chem.*, 2019, **62**(6), 3009–3020, DOI: **10.1021/acs.jmedchem.8b01822**.

40 F. Riefolo, C. Matera, A. Garrido-Charles, A. M. J. Gomila, R. Sortino, L. Agnetta, E. Claro, R. Masgrau, U. Holzgrabe, M. Batlle, M. Decker, E. Guasch and P. Gorostiza, Optical Control of Cardiac Function with a Photoswitchable Muscarinic Agonist, *J. Am. Chem. Soc.*, 2019, **141**(18), 7628–7636, DOI: **10.1021/jacs.9b03505**.

41 *EP* 2322171 *A2* 20110518 – *Fluorine labeled L-glutamic acid derivatives*. **https://data.epo.org/gpi/EP2322171A2** (accessed 2024-03-11).

42 M. Bose, D. Groff, J. Xie, E. Brustad and P. G. Schultz, The Incorporation of a Photoisomerizable Amino Acid into Proteins in E. Coli, *J. Am. Chem. Soc.*, 2006, **128**(2), 388–389, DOI: **10.1021/ja055467u**.

43 W. Li, I. Park, S.-K. Kang and M. Lee, Smart Hydrogels from Laterally-Grafted Peptide Assembly, *Chem. Commun.*, 2012, **48**(70), 8796–8798, DOI: **10.1039/C2CC34528E**.

44 S. Mukherjee and D. Manahan-Vaughan, Role of Metabotropic Glutamate Receptors in Persistent Forms of Hippocampal Plasticity and Learning, *Neuropharmacology*, 2013, **66**, 65–81, DOI: **10.1016/j.neuropharm.2012.06.005**.

45 M. Izquierdo-Serra, A. Bautista-Barrufet, A. Trapero, A. Garrido-Charles, A. Díaz-Tahoces, N. Camarero, S. Pittolo, S. Valbuena, A. Pérez-Jiménez, M. Gay, A. García-Moll, C. Rodríguez-Escrich, J. Lerma, P. de la Villa, E. Fernández, M.À Pericàs and A. Llebaria, Gorostiza, P. Optical Control of Endogenous Receptors and Cellular Excitability Using Targeted Covalent Photoswitches, *Nat. Commun.*, 2016, **7**(1), 12221, DOI: **10.1038/ncomms12221**.

46 A. Garrido-Charles, A. Huet, C. Matera, A. Thirumalai, J. Hernando, A. Llebaria, T. Moser and P. Gorostiza, Fast Photoswitchable Molecular Prosthetics Control Neuronal Activity in the Cochlea, *J. Am. Chem. Soc.*, 2022, **144**(21), 9229–9239, DOI: **10.1021/jacs.1c12314**.

47 J. Levitz, J. Broichhagen, P. Leippe, D. Konrad, D. Trauner and E. Y. Isacoff, Dual Optical Control and Mechanistic Insights into Photoswitchable Group II and III Metabotropic Glutamate Receptors, *Proc. Natl. Acad. Sci. U. S. A.*, 2017, **114**(17), E3546–E3554, DOI: **10.1073/pnas.1619652114**.

48 G. Cabré, A. Garrido-Charles, M. Moreno, M. Bosch, M. Porta-de-la-Riva, M. Krieg, M. Gascón-Moya, N. Camarero, R. Gelabert, J. M. Lluch, F. Busqué, J. Hernando, P. Gorostiza and R. Alibés, Rationally Designed Azobenzene Photoswitches for Efficient Two-Photon Neuronal Excitation, *Nat. Commun.*, 2019, **10**(1), 907, DOI: **10.1038/s41467-019-08796-9**.

49 F. Riefolo, R. Sortino, C. Matera, E. Claro, B. Preda, S. Vitiello, S. Traserra, M. Jiménez and P. Gorostiza, Rational Design of Photochromic Analogues of Tricyclic Drugs, *J. Med. Chem.*, 2021, **64**(13), 9259–9270, DOI: **10.1021/acs.jmedchem.1c00504**.

50 R. Sortino, M. Cunquero, G. Castro-Olvera, R. Gelabert, M. Moreno, F. Riefolo, C. Matera, N. Fernàndez-Castillo, L. Agnetta, M. Decker, J. M. Lluch, J. Hernando, P. Loza-Alvarez and P. Gorostiza, Three-Photon Infrared Stimulation of Endogenous Neuroreceptors in Vivo, *Angew. Chem., Int. Ed.*, 2023, **62**(51), e202311181, DOI: **10.1002/anie.202311181**.

51 V. Voliani, G. Signore, O. Vittorio, P. Faraci, S. Luin, J. Peréz-Prieto and F. Beltram, Cancer Phototherapy in Living Cells by Multiphoton Release of Doxorubicin from Gold Nanospheres, *J. Mater. Chem. B*, 2013, **1**(34), 4225–4230, DOI: **10.1039/C3TB20798F**.

52 B. M. Borah, J. Cacaccio, R. Watson and R. K. Pandey, Phototriggered Release of Tumor-Imaging and Therapy Agents from Lyophilized Multifunctional Polyacrylamide Nanoparticles, *ACS Appl. Bio Mater.*, 2019, **2**(12), 5663–5675, DOI: **10.1021/acsabm.9b00741**.

53 S. Biswas, R. Mengji, S. Barman, V. Venugopal, A. Jana and N. D. P. Singh, 'AIE + ESIPT' Assisted Photorelease: Fluorescent Organic Nanoparticles for Dual Anticancer Drug Delivery with Real-Time Monitoring Ability, *Chem. Commun.*, 2017, **54**(2), 168–171, DOI: **10.1039/C7CC07692D**.

54 D. Liu, S. Wang, S. Xu and H. Liu, Photocontrollable Intermittent Release of Doxorubicin Hydrochloride from Liposomes Embedded by Azobenzene-Contained Glycolipid, *Langmuir*, 2017, **33**(4), 1004–1012, DOI: **10.1021/acs.langmuir.6b03051**.

55 B. Lu, G. Zhou, F. Xiao, Q. He and J. Zhang, Stimuli-Responsive Poly(Ionic Liquid) Nanoparticles for Controlled Drug Delivery, *J. Mater. Chem. B*, 2020, **8**(35), 7994–8001, DOI: **10.1039/D0TB01352H**.

56 S. Yadav, S. R. Deka, G. Verma, A. K. Sharma and P. Kumar, Photoresponsive Amphiphilic Azobenzene–PEG Self-Assembles to Form Supramolecular Nanostructures for Drug Delivery Applications, *RSC Adv.*, 2016, **6**(10), 8103–8117, DOI: **10.1039/C5RA26658K**.

57 D. K. Prusty, V. Adam, R. M. Zadegan, S. Irsen and M. Famulok, Supramolecular Aptamer Nano-Constructs for Receptor-Mediated Targeting and Light-Triggered Release of Chemotherapeutics into Cancer Cells, *Nat. Commun.*, 2018, **9**(1), 535, DOI: **10.1038/s41467-018-02929-2**.

58 J. Hatai, C. Hirschhäuser, J. Niemeyer and C. Schmuck, Multi-Stimuli-Responsive Supramolecular Polymers Based on Noncovalent and Dynamic Covalent Bonds, *ACS Appl. Mater. Interfaces*, 2020, **12**(2), 2107–2115, DOI: **10.1021/acsami.9b19279**.

59 V. Torchilin, Tumor Delivery of Macromolecular Drugs Based on the EPR Effect, *Adv. Drug Delivery Rev.*, 2011, **63**(3), 131–135, DOI: **10.1016/j.addr.2010.03.011**.

60 M. Zheng and J. Yuan, Polymeric Nanostructures Based on Azobenzene and Their Biomedical Applications: Synthesis, Self-Assembly and Stimuli-Responsiveness, *Org. Biomol. Chem.*, 2022, **20**(4), 749–767, DOI: **10.1039/D1OB01823J**.

61 M. Dong, A. Babalhavaeji, S. Samanta, A. A. Beharry and G. A. Woolley, Red-Shifting Azobenzene Photoswitches for in Vivo Use, *Acc. Chem. Res.*, 2015, **48**(10), 2662–2670, DOI: **10.1021/acs.accounts.5b00270**.

62 A. Kerckhoffs, Z. Bo, S. E. Penty, F. Duarte and M. J. Langton, Red-Shifted Tetra-Ortho-Halo-Azobenzenes for Photo-Regulated Transmembrane Anion Transport, *Org. Biomol. Chem.*, 2021, **19**(41), 9058–9067, DOI: **10.1039/D1OB01457A**.

63 M. J. Hansen, M. M. Lerch, W. Szymanski and B. L. Feringa, Direct and Versatile Synthesis of Red-Shifted Azobenzenes, *Angew. Chem., Int. Ed.*, 2016, **55**(43), 13514–13518, DOI: **10.1002/anie.201607529**.